Author/s:
Bedggood, P;Tanabe, F;McKendrick, AM;Turpin, A;Anderson, AJ;Bui, BV

Title:
Optic nerve tissue displacement during mild intraocular pressure elevation: its relationship to central corneal thickness and corneal hysteresis

Date:
2018-07-01

Citation:
Bedggood, P., Tanabe, F., McKendrick, A. M., Turpin, A., Anderson, A. J. & Bui, B. V. (2018). Optic nerve tissue displacement during mild intraocular pressure elevation: its relationship to central corneal thickness and corneal hysteresis. Ophthalmic and Physiological Optics, 38 (4), pp.389-399. https://doi.org/10.1111/opo.12568.

Persistent Link:
https://hdl.handle.net/11343/284073

DR. PHILLIP BEDGGOOD (Orcid ID : 0000-0001-5144-3694)

DR. ALLISON MCKENDRICK (Orcid ID : 0000-0003-1972-1222)

DR. ANDREW ANDERSON (Orcid ID : 0000-0001-7015-0061)

Article type : Original Article

Title: Optic nerve tissue displacement during mild IOP elevation: its relationship to central corneal thickness and corneal hysteresis

Running Head: ONH displacement with mild IOP elevation

Authors

Phillip Bedggood[1], Fumi Tanabe[2], Allison M McKendrick[1], Andrew Turpin[3], Andrew J Anderson[1], Bang V Bui[1,*].

Affiliations

[1]Department of Optometry and Vision Sciences, The University of Melbourne, Parkville, Australia

[2]Department of Ophthalmology, Kindai University Faculty of Medicine, Osaka-Sayama, Japan

[3]School of Computing and Information Systems, The University of Melbourne, Parkville, Australia

Correspondence

Bang Viet Bui
Email: bvb@unimelb.edu.au

Key words
ophthalmodynamometry; optic nerve head; intraocular pressure; biomechanics

Abstract

Purpose: To determine the extent to which a) optic nerve tissue is displaced following mild acute elevation of intraocular pressure, and b) clinically accessible measures at the anterior eye can be used as a surrogate for such displacements.

Methods: We imaged the optic disc of 21 healthy subjects before and after IOP elevation of ~10 mmHg delivered by ophthalmodynamometry. Steady-state tissue displacement during IOP elevation was assessed axially from OCT data, and laterally from SLO data. Recovery from IOP elevation was assessed by tracking a single vertical B-scan through the cup centre. Anatomical structures were demarcated by three masked clinicians to determine lateral shifts for temporal cup edge and central disc vessels, and axial shifts of disc surface and anterior lamina cribrosa. Spatial maps of deformation were constructed within the demarcated cup and disc to assess within-tissue displacement. Measured displacements were correlated with corneal hysteresis, corneal thickness, and IOP.

Results: The temporal cup edge moved more temporally with higher baseline IOP (R^2=0.33, p=0.006) and with lesser elevation of IOP (R^2=0.43, p=0.001); it moved more superiorly for thinner corneas (R^2=0.35, p=0.007). Thinner corneas also produced less within-cup deformation, relative to that of the disc (R^2=0.39, p=0.004). Axial displacement of the lamina and lateral displacement of vessels were often substantial (lamina 20±15 μm, range 1-60 μm; vessels 37±25 μm, range 2-102 μm) but did not correlate with measured parameters. Recovery from IOP elevation did not take more than 300-400 ms in any subject.

Conclusions: Mild acute elevation of IOP produces large and rapidly reversible shifts in optic nerve tissue in young, healthy eyes. The resulting degree, direction and spatial distribution of cup movement are associated with IOP status and corneal thickness, but not corneal hysteresis.

INTRODUCTION

The biomechanical properties of the peripapillary sclera and the lamina cribrosa are thought to influence the susceptibility of ganglion cell axons to injury associated with elevation of intraocular pressure (IOP).[1, 2] Deformation of the lamina pores with IOP elevation can lead to increased stress and strain on the ganglion cell axons as they pass though the lamina cribrosa.[3] Additionally, connective tissue deformation can activate optic nerve head astrocytes, altering their interactions with axons, the vasculature and connective tissues.[4]

Examining how changes in IOP modify the shape of the optic nerve head can provide information about these important biomechanical properties. Several recent studies have done this using methods that include *ex vivo* eye preparations,[5] *in vivo* IOP elevation in animals,[6] and direct visualisation of IOP induced changes in human subjects [7]. For example, Fazio et al.[8] reported that greater tissue displacement with IOP elevation was associated with older age and African descent. Some studies have linked these changes to functional deficits; for example, greater transient IOP-induced thinning of the inferotemporal neuroretinal rim is associated with more severe visual field defect in the corresponding sector.[9] Others have sought to assess the effect of IOP lowering on optic nerve structures in glaucomatous eyes.[10, 11] Of interest, those with greater visual field deficits tended to show less lamina cribrosa displacement [12] and greater local lamina cribrosa strain [13] in response to IOP lowering. Whilst such customised testing provides useful biomechanical insights, it would be highly desirable if simple, existing clinical measures could also be shown to predict biomechanical properties of the optic nerve head. This could open the possibility of identifying in the clinic those patients with unusual biomechanical properties which might make them more susceptible to damage from elevated IOP.

Given that they make up the outer shell of the eye, investigators have sought to correlate characteristics of the cornea, sclera and lamina cribrosa. Although studies have found that central corneal thickness and lamina cribrosa thickness are poorly related,[14 15] such measures provide limited information about tissue biomechanical properties.

More recent studies have attempted to examine the relationship between corneal and optic nerve responses to pressure-related stress. Amongst readily available measures, corneal hysteresis (CH) provides an index of the energy absorption characteristics of the cornea, and has been shown to be associated with both structural and functional loss in glaucoma. For example, multivariate data analysis by Vu et al.[16] revealed corneal hysteresis to be

independently associated with visual field mean defect, whilst parameters such as vertical cup to disc ratio, rim area and age were not. Studies also report that lower corneal hysteresis is associated with greater likelihood of glaucomatous visual field loss and faster rates of retinal nerve fibre layer thinning.[17, 18] In addition, lower corneal hysteresis has been associated with greater cupping.[19] In terms of biomechanical properties, Lanzagorta-Aresti et al.[20] examined the effect of medical IOP lowering (~7 mmHg) on lamina cribrosa position in patients with ocular hypertension or elevated IOP due to glaucoma. They found there was greater change in lamina cribrosa position in those who were younger and had higher corneal hysteresis.

It is not clear, however, that biomechanical changes after the removal of chronic IOP elevation will be equivalent to those following an IOP increase. However, it is presumably the eye's response to an IOP increase that is of most direct importance in the pathogenesis of glaucomatous damage. In addition, Lanzagorta-Aresti et al.[20] only measured biomechanical changes (lamina thickness, lamina displacement, pre-lamina tissue thickness, pre-lamina tissue displacement) for a central location on the optic nerve head. It may be that significant structural changes occur at non-central locations, or laterally as opposed to in depth.

Wells et al.[21] have sought to more directly examine the relationship between corneal hysteresis and the biomechanical properties of the optic nerve as IOP increases. Using scanning laser ophthalmoscopy to map the surface of the optic disc before and after acute IOP elevation, they showed that greater optic nerve surface displacement was correlated with higher corneal hysteresis, but not with central corneal thickness. However, the IOP levels used in that study were extreme (an average of 65 mmHg) and so are less representative of what an eye might typically encounter in primary open angle glaucoma. Other studies have explored more modest IOP elevations, but did not consider biomechanical properties manifest in measurements of corneal thickness and hysteresis.[22-24] Furthermore, previous studies have not examined whether differences in the time course of IOP-induced tissue displacements may biomechanically distinguish eyes, even if the overall magnitude of the displacement between eyes is the same.

The aim of the present study was to consider the relationship between central corneal thickness, corneal hysteresis and optic nerve displacement induced by a mild, acute IOP elevation comparable in size to chronic IOP elevations often encountered in open angle

glaucoma. To this end we employed a) vertical optical coherence tomography (OCT) scans through the optic nerve to both measure axial displacement, and to provide high temporal resolution for tracking the time course of recovery upon removal of IOP elevation; and b) infrared scanning laser ophthalmoscopy (SLO) to measure lateral displacement of optic nerve tissue. We hypothesised that the following factors would be associated with more tissue deformation; higher baseline IOP, a larger change in IOP, thicker cornea and higher corneal hysteresis.

METHODS

Overview

The optic nerve head of healthy subjects was imaged before and after acute elevation of IOP. The target elevation was +10 mmHg, whilst a separate experimental run with the device targeting +0 mmHg gave a baseline. The time course of events is shown in Figure 1. Force was applied with an ophthalmodynamometer to give steady state IOP elevation (20 sec), which was maintained for subsequent acquisition of OCT cube data (30 sec). The same force was maintained for a further 50 sec, during which time data was saved and the device reconfigured to acquire rapid single B-scans at the disc to monitor recovery (10 sec). Acquired OCT and SLO data were manually assessed by three masked graders to quantify displacement of key anatomical structures. Tissue displacements were assessed for correlation with corneal hysteresis, central corneal thickness, axial length and IOP to determine how well these parameters predicted tissue displacement.

Experimental participants

21 healthy participants were recruited from staff and students in the Department of Optometry and Vision Sciences at the University of Melbourne. All participants provided written informed consent prior to participation in accordance with a protocol approved by the Human Research Ethics Committee of the University of Melbourne and compliant with the tenets of the Declaration of Helsinki. The left eye from each participant was used.

Basic testing

Each participant underwent a full eye examination. All participants had visual acuity better than 6/9.5 (0.2 logMAR, ~20/30) in the tested eye (measured after subjective refraction), spherical refractive error between −12 dioptres (D) and +6 D, astigmatism no greater than −2 D, and no significant ocular pathology. Risk factors for glaucoma such as large cup-disc ratio, baseline IOP >= 21 mmHg, or high axial length were not specifically excluded, since they may yield useful information on optic nerve biomechanics. However, all participants showed both minimum rim width and peripapillary retinal nerve fibre layer thickness to be within normative limits with the Heidelberg Spectralis Glaucoma Module (https://business-lounge.heidelbergengineering.com/us/en/products/spectralis/glaucoma-module/).

IOP was measured with an iCare TA01i rebound tonometer (https://www.icaretonometer.com/products/icare-ta01/), taking the median of five measurements acquired within 10 seconds. Axial length was measured using A-scan ultrasound biometry (https://tomey.de/en/products/ultrasound/al-100), with the average of three individual measures taken. Central corneal thickness (CCT) was measured by pachymetry (http://dghtechnology.com/product/pachmate/), with the final estimate being the average of at least three repeated measures per eye. Corneal hysteresis (CH) was measured with an Ocular Response Analyzer G3 (http://www.reichert.com/product_details.cfm?skuId=2976&skuTk=1036239258).

Steady-state image acquisition

Image data were acquired with a Heidelberg Spectralis (https://business-lounge.heidelbergengineering.com/us/en/products/spectralis/), which produced both OCT and SLO data.

Optical coherence tomography with enhanced depth imaging (EDI) produced cubes of extent $10x15^0$ (horizontal x vertical), with vertical B-scans 0.21^0 apart (~60 µm). Each B-scan was the average of 9 individual scans (ART setting). Scans were manually centred on the optic nerve head and oriented vertically. Acquisition time was ~30 sec and signal strength > 25 dB for all participants. OCT data were compared for target IOP elevation of either +10 mmHg or +0 mmHg to determine axial displacement of optic nerve tissue resulting from IOP elevation.

At the beginning of each OCT cube acquisition, the Spectralis also acquires an infrared scanning laser ophthalmoscopy (SLO) image of the fundus. SLO data were compared between +10 mmHg and +0 mmHg conditions to determine lateral displacement of optic nerve tissue.

In addition to force and baseline conditions, an initial set of reference images was acquired, with the ophthalmodynamometer not in contact with the eye. This minimized distortion of the globe in order to maximize image quality. Each initial image was set as a reference for image registration using the software's standard follow-up feature, so that subsequent scans in the same eye were automatically acquired in the same position.

Recovery image acquisition

Following acquisition of steady-state images described above, time course of recovery was assessed using a single vertical B-scan placed manually at the deepest portion of the optic cup. The dimensions and orientation of this B-scan were identical to those of the cube described above, to allow easy comparison. Each B-scan was the average of four individual B-scans, which improved image quality at the expense of frame rate (9.8 fps).

Ophthalmodynamometry

The ophthalmodynamometer was a custom device (http://www.ubiquitus.com.au/) consisting of a 6 mm diameter rounded probe applied to the lower lid at 45-degrees below horizontal, driven by a computer controlled linear motor, with force maintained automatically via feedback from a pressure sensor on which the probe was mounted. Our approach to IOP elevation could potentially produce focal distortion of the globe; an expected outcome of this would be a measurable change in astigmatic refraction and decrease in visual acuity. However for a subsample of our participants (n = 5) we measured these parameters before and during IOP elevation, and found no difference in cylindrical refraction (baseline: 0.27 ± 0.51 DC vs. IOP elevation: 0.19 ± 0.46 DC; p = 0.19) nor in visual acuity (baseline: 0.13 ± 0.06 logMAR vs. IOP elevation: 0.11 ± 0.06 logMAR, p = 0.2). Thus, we consider the influence of any focal distortion of the globe to be negligible in this study.

To set the correct target force, an initial calibration was applied for each participant by increasing force in steps of 50 mN until the target elevation was reached (+10 mmHg, typically with force at 300-400 mN). Actual IOP elevations achieved in the subsequent experimental runs were 12.0 ± 4.2 mmHg (range 6.5 to 22.0 mmHg). For comparison, 95%

limits of agreement were ± 3.90 mmHg between IOP at zero force and IOP with the probe removed altogether. This compares favourably to previously reported figures for rebound tonometry (5.11 mmHg) and Goldmann tonometry (3.15 mmHg). [25] Therefore, much of the spread in IOP elevations likely resulted from variation in positioning of the probe and the discrete force increments trialled, rather than measurement error.

Main procedure

Two experimental runs were conducted. The first run was a baseline run (target force 0 mN), and the second used the target force determined above. Each run produced one SLO fundus image, one OCT volume, and one movie of OCT recovery (single B-scan over time). The time course of events is shown in Figure 1. Runs were aborted if change in IOP was <5 mmHg or if OCT image quality was deemed insufficient.

Manual grading of steady-state image data

Image data were exported from Heidelberg Eye Explorer version 6.3, in .vol format, and imported to Matlab R2015b (https://www.mathworks.com/products/matlab.html) to generate images for masked human graders to assess.

For the OCT volumes, we analysed the same slice through the optic nerve head in each condition (+0 mmHg, +10 mmHg, and recovery). This was achieved by finding the B-scan from the baseline OCT cube which was closest in physical location to the single B-scan of the recovery movie. The same numbered B-scan was selected from the +0 mmHg and +10 mmHg conditions, and these two B-scans were passed to masked graders. The IR SLO images, acquired at the beginning of each cube, were also passed to masked graders.

Grading was carried out by experienced clinicians, using Adobe Photoshop CS6 (https://www.adobe.com/au/products/photoshop.html) to trace single-pixel lines demarcating each structure. Based on initial assessment of the displacements evident in our data, we chose to assess lateral displacement for the central disc vessels (which bound the cup nasally) and for the temporal edge of the cup. Axially, we assessed displacement of the disc surface and the anterior lamina cribrosa (see below for details). Graders were instructed to grade both (masked +0 and +10 mmHg) images side-by-side, to ensure no change between conditions in the subjective criterion adopted to differentiate structures.

Automated analysis based on manual grading

Graded images were imported to Matlab for analysis with custom software. Overall displacement of structures was calculated by cross-correlation of the binary traces between the +0 mmHg and +10 mmHg conditions, producing the x, y shifts required to best align the two traces.

To emphasize relative shifts which could place strain on tissue, lateral movements (vessels and cup edge) were referenced to movement of the disc, whilst axial movements (disc surface and anterior lamina) were referenced to Bruch's membrane 1500 µm from the disc centre. Because demarcation of the lamina was difficult in our data, we restricted the calculation of axial displacements to the deepest part of the cup, where contrast is generally higher.

In addition to whole-structure shifts, we calculated within-structure deformation using the "demons" diffeomorphic image registration algorithm in Matlab 2015b Image Processing Toolbox, with default settings. This algorithm treats image boundaries as semi-permeable membranes through which information can "diffuse" in order to best match a reference image.[26] The output is a map of local x- and y-shifts which allow one image to be warped to resemble another; possible warping includes lateral shifts, rotations, and apparent size change of structures. The resulting deformation maps were calculated for the disc (lateral and axial data) and for the visible cup (lateral data). Examples are shown in the Results section. Analysis was restricted to a region of interest 512 pixels wide (approx. 2960 µm, or twice the average horizontal diameter of the disc) centred on the optic nerve head. Image histograms were first matched to each other using the Matlab “imhistmatch” function.

Grading of recovery movie

Initial inspection of recovery movies showed that the deepest portion of the cup rebounded very quickly under our experimental conditions, i.e. after no more than 3-4 frames (~300-400 ms according to the reported frame rate in the Spectralis software) in all observers. We therefore performed no further quantitative analysis given the lack of temporal resolution in our data to distinguish recovery time-course differences between eyes. A representative example recovery movie is shown in Supporting Information 1.

RESULTS

Demographic parameters of our study population are given in Table 1. Our ophthalmodynamometer produced a statistically significant increase in IOP that was close to our target of +10 mmHg.

As has been previously reported we found that those with thicker central corneas tend to have higher corneal hysteresis (Figure 2A) and higher IOP (Figure 2B). There was no relationship between corneal hysteresis and baseline IOP level.

Figures 3A and 3B shows representative infrared SLO images of the optic nerve head at baseline and during IOP elevation. We assessed the extent of displacement of the vessel edge and the cup edge both in the horizontal and vertical directions, and expressed this relative to the horizontal and vertical displacement of the entire disc, respectively.

Table 2 summarises the correlations for all parameters. Values in red were statistically significant ($p<0.05$). It should be noted that this table represents 47 individual correlations; at an alpha level of 0.05 we might expect 2 of these to be significant due to chance alone, however, we did not apply a correction for multiple comparisons due to the exploratory nature of the study.[27] The 4 strongest correlations relating to the SLO parameters are shown in Figure 3 (C - F).

Intraocular pressure and tissue displacement

Figure 3C shows that higher baseline IOP was associated with displacement of the cup edge temporally during mild IOP elevation. A lower baseline IOP was significantly associated with nasal displacement during IOP elevation. There were no other significant association between baseline IOP and other parameters (Table 2).

A significant relationship was also noted with the level of IOP elevation (Figure 3D). Higher IOP elevation produced more nasal displacement of the cup edge. No such correlation was noted between the level of IOP elevation and displacement of the vessel edge (Table 2).

Central corneal thickness, corneal hysteresis and tissue displacement

A thicker central cornea was associated with a more inferior displacement of the cup edge after IOP elevation (Figure 3E). Corneal hysteresis was poorly correlated to our SLO parameters of optic nerve head tissue displacement. Figure 3F shows the strongest

association of any parameter with corneal hysteresis, which was vertical displacement of the vessel edge. However, this was not significant (p=0.12).

Optic nerve displacement maps

Displacement maps were developed for each set of *en face* images of the nerve head. Two regions of interest were demarcated: the whole disc (encompassed by the traced disc margins) and the visible cup (bounded temporally by the traced cup edge and nasally by the traced vessels). The average displacement within the cup was then expressed as a ratio of that across the entire disc. Diffuse (non-localized) displacement of the tissue would result in a ratio close to 1 (values given in the upper right corner of maps in Figure 4A).

Figure 4A shows example displacement maps from six subjects. Whilst the IOP achieved was similar in these examples, the extent and patterns of displacement can vary markedly between individuals.

There were no significant correlations between within-disc displacement and any of our baseline parameters or IOP elevation (Table 2). When we expressed the amount of cup displacement relative to the entire disc, there was a significant association between having a thicker central cornea and showing more cup displacement relative to the entire disc (i.e. a higher ratio as shown in Figure 4C).

Tissue displacement assessed using OCT

Representative examples of vertically oriented OCT B-scans from one subject at baseline (Figure 5A) and during IOP elevation (Figure 5B) illustrate the subtle effects of mild IOP elevation on optic nerve tissues. We found no significant relationship between central corneal thickness and displacement of the anterior lamina (Figure 5C). Likewise, there was no significant relationship between corneal hysteresis and anterior lamina cribrosa displacement (Figure 5D; Table 2).

We also considered relationships between IOP-induced displacement detected using SLO and OCT on the same eyes. We found a statistically significant relationship between greater IOP-induced posterior displacement of the anterior lamina cribrosa, and inferior displacement of the cup edge (Figure 5E). No such relationship was found between displacement of the lamina and displacement of the vessels (Figure 5F).

DISCUSSION

We show that mild transient IOP elevation produces lateral displacement in the cup and large central vessels, as well as axial displacement of the optic nerve surface and anterior lamina cribrosa [23, 24]. Unlike Wells et al.[21] we did not find a significant correlation between higher corneal hysteresis and displacement of the optic nerve surface during transient elevations of IOP. However, the levels of IOP elevation employed in that study were substantially higher than that used here, thus high IOP levels may be needed to reveal a relationship with corneal hysteresis. Our study considered mild acute IOP elevations that might be normally encountered on a more regular basis, and are more comparable in magnitude to chronic elevations typically encountered in primary open angle glaucoma. We did find that eyes with thicker central cornea showed vertical displacement of the cup edge (Figure 3E), suggesting the optic nerve in these eyes to be more compliant and hence better able to cope with mild transient IOP elevations.

We found levels of lamina and pre-laminar (optic nerve surface) displacement of a similar magnitude to Agoumi et al.[22], who employed similar levels of IOP elevation. Interestingly, Agoumi et al. reported that the anterior lamina cribrosa underwent little displacement, whereas the pre-laminar tissue showed more displacement. The authors also reported that the amount of pre-laminar displacement was associated with higher levels of IOP elevation. Whilst we did not find such a correlation, we did find that higher IOP produced more nasal cup displacement (Figure 3D). This may be caused in part by expansion of the scleral canal in response to IOP elevation, which has been found to pull the lamina cribrosa taut.[28]

Using a serial sectioning approach Sigal et al.[29] showed that displacements of the vitreo-retinal interface and the anterior surface of the lamina cribrosa varied substantially between individuals. Their modelling attributed the biggest influence on inter-subject differences to differences in tissue stiffness, particularly of the sclera, whilst differences in tissue geometry had much less influence. This may be consistent with our finding that there was a significant association between central corneal thickness and cup displacement. Specifically, those with thicker central cornea tended to show more downward displacement of the cup in response to IOP elevation (Figure 3E). Thicker central cornea was also correlated with more localised cup displacement (Figure 4C). These findings support the general idea that central corneal thickness may serve as a surrogate for tissue material properties.

Some of our largest tissue displacements were observed in the lateral dimension, i.e. from the SLO images. These displacements were relatively easy to visualize and were correlated with biometric parameters as discussed above, suggesting possible clinical utility in the future. In comparison, axial displacement of the lamina cribrosa was difficult to assess in our images due to poor visibility, and was not correlated with biometric parameters. However, our single analysed vertical B-scan may have missed displacement elsewhere in the tissue, and differences in imaging hardware and post processing may allow improved visualization of the anterior lamina cribrosa in many subjects.[30] Thus, more comprehensive OCT data and analysis may reveal stronger relationships between axial changes and biometric parameters.

Within-tissue lateral displacement maps revealed robust displacement that varied substantially between individuals both in pattern and in magnitude. Broadly, the pattern of displacement fell into those that show little or diffuse displacement across the entire disc, as well as those for whom IOP elevation produced more displacement within the cup. Those with thicker central corneas tended to fall into the latter category (Figure 4C), with direction of movement biased inferiorly (Figure 3E). It is of interest that in some of subjects we saw highly localised areas of deformation (Figure 4A, upper middle and lower left examples). These results suggest that in addition to the magnitude of displacement, there may be useful information to be gained in differentiating patients that show diffuse compared with more focal deformation in response to IOP elevation [9]. It should be noted that measured deformations could be affected in some way as a result of unknown tracking and registration methods employed by proprietary OCT software, even though software settings for imaging were kept constant. Additionally, the relatively focal nature of our force application could confer a small amount of focal tension through the sclera to the optic nerve.

An unexpected finding of this study was the rapid recovery of tissue displacement following withdrawal of IOP elevation. Even though we employed a single B-scan to maximize frame rate (9.8 fps), the tissue recovered in only 3-4 frames (~300-400 ms), meaning that no meaningful differences between individuals could be extracted. It may be fruitful to revisit this issue with higher frame rate imaging and/or larger IOP elevations in the future. One potential additional metric of interest would be any hysteresis in the optic nerve structures themselves (rather than using corneal hysteresis as a surrogate), which could be assessed

by determining how closely the tissue returns to the same position after repeated elevation/withdrawal of IOP.

CONCLUSIONS

We have shown that there are significant lateral shifts in tissues of the optic nerve in response to a mild transient IOP elevation in normal eyes. Such shifts recovered in less than one second. Although corneal hysteresis has been previously found to be predictive of the biomechanical response of the optic nerve head to extreme IOP elevation (>60 mmHg), we do not find this to be the case for acute elevations closer in magnitude to that of chronic elevations expected in open angle glaucoma. Thicker corneas, on the other hand, were correlated with vertical cup movement and with more focal localisation of deformation within the cup. Given these positive results for healthy, younger eyes, there appears some merit to exploring a similar protocol in older eyes and those with glaucoma or ocular hypertension.

DISCLOSURE

Authors McKendrick and Turpin received financial support from Heidelberg Engineering GmBH.

ACKNOWLEDGEMENTS

This work was supported by Australian Research Council Future Fellowship FT130100338 and Australian Research Council Linkage Project ARC LP130100055.**REFERENCES**

1. Burgoyne CF, Downs JC, Bellezza AJ, Suh JK, Hart RT. The optic nerve head as a biomechanical structure: a new paradigm for understanding the role of IOP-related stress and strain in the pathophysiology of glaucomatous optic nerve head damage. *Prog Retin Eye Res* 2005;24:39-73.
2. Downs JC, Blidner RA, Bellezza AJ, Thompson HW, Hart RT, Burgoyne CF. Peripapillary scleral thickness in perfusion-fixed normal monkey eyes. *Invest Ophthalmol Vis Sci* 2002;43:2229-2235.
3. Sigal IA, Flanagan JG, Tertinegg I, Ethier CR. Predicted extension, compression and shearing of optic nerve head tissues. *Exp Eye Res* 2007;85:312-322.
4. Schneider M, Fuchshofer R. The role of astrocytes in optic nerve head fibrosis in glaucoma. *Exp Eye Res* 2016;142:49-55.

5. Sigal IA, Grimm JL, Jan NJ, Reid K, Minckler DS, Brown DJ. Eye-specific IOP-induced displacements and deformations of human lamina cribrosa. *Invest Ophthalmol Vis Sci* 2014;55:1-15.
6. Ivers KM, Yang H, Gardiner SK, et al. In Vivo Detection of laminar and peripapillary scleral hypercompliance in early monkey experimental glaucoma. *Invest Ophthalmol Vis Sci* 2016;57:OCT388-403.
7. Balaratnasingam C, Morgan WH, Hazelton ML, et al. Value of retinal vein pulsation characteristics in predicting increased optic disc excavation. *Br J Ophthalmol* 2007;91:441-444.
8. Fazio MA, Johnstone JK, Smith B, Wang L, Girkin CA. Displacement of the lamina cribrosa in response to acute intraocular pressure elevation in normal individuals of African and European descent. *Invest Ophthalmol Vis Sci* 2016;57:3331-3339.
9. Tun TA, Atalay E, Baskaran M, et al. Association of functional loss with the biomechanical response of the optic nerve head to acute transient intraocular pressure elevations. *JAMA Ophthalmol* 2018.
10. Irak I, Zangwill L, Garden V, Shakiba S, Weinreb RN. Change in optic disk topography after trabeculectomy. *Am J Ophthalmol* 1996;122:690-695.
11. Lesk MR, Spaeth GL, Azuara-Blanco A, et al. Reversal of optic disc cupping after glaucoma surgery analyzed with a scanning laser tomograph. *Ophthalmology* 1999;106:1013-1018.
12. Quigley H, Arora K, Idrees S, et al. Biomechanical responses of lamina cribrosa to intraocular pressure change assessed by optical coherence tomography in glaucoma eyes. *Invest Ophthalmol Vis Sci* 2017;58:2566-2577.
13. Girard MJ, Beotra MR, Chin KS, et al. In vivo 3-dimensional strain mapping of the optic nerve head following intraocular pressure lowering by trabeculectomy. *Ophthalmology* 2016;123:1190-1200.
14. Jonas JB, Holbach L. Central corneal thickness and thickness of the lamina cribrosa in human eyes. *Invest Ophthalmol Vis Sci* 2005;46:1275-1279.
15. Omodaka K, Takahashi S, Matsumoto A, et al. Clinical factors associated with lamina cribrosa thickness in patients with glaucoma, as measured with swept source optical coherence tomography. *PLoS One* 2016;11:e0153707.
16. Vu DM, Silva FQ, Haseltine SJ, Ehrlich JR, Radcliffe NM. Relationship between corneal hysteresis and optic nerve parameters measured with spectral domain optical coherence tomography. *Graefes Arch Clin Exp Ophthalmol* 2013;251:1777-1783.

17. Park JH, Jun RM, Choi KR. Significance of corneal biomechanical properties in patients with progressive normal-tension glaucoma. *Br J Ophthalmol* 2015;99:746-751.
18. Zhang C, Tatham AJ, Abe RY, et al. Corneal hysteresis and progressive retinal nerve fiber layer loss in glaucoma. *Am J Ophthalmol* 2016;166:29-36.
19. Prata TS, Lima VC, de Moraes CG, et al. Factors associated with topographic changes of the optic nerve head induced by acute intraocular pressure reduction in glaucoma patients. *Eye (Lond)* 2011;25:201-207.
20. Lanzagorta-Aresti A, Perez-Lopez M, Palacios-Pozo E, Davo-Cabrera J. Relationship between corneal hysteresis and lamina cribrosa displacement after medical reduction of intraocular pressure. *Br J Ophthalmol* 2017;101:290-294.
21. Wells AP, Garway-Heath DF, Poostchi A, Wong T, Chan KC, Sachdev N. Corneal hysteresis but not corneal thickness correlates with optic nerve surface compliance in glaucoma patients. *Invest Ophthalmol Vis Sci* 2008;49:3262-3268.
22. Agoumi Y, Sharpe GP, Hutchison DM, Nicolela MT, Artes PH, Chauhan BC. Laminar and prelaminar tissue displacement during intraocular pressure elevation in glaucoma patients and healthy controls. *Ophthalmology* 2011;118:52-59.
23. Azuara-Blanco A, Harris A, Cantor LB, Abreu MM, Weinland M. Effects of short term increase of intraocular pressure on optic disc cupping. *Br J Ophthalmol* 1998;82:880-883.
24. Piette S, Liebmann JM, Ishikawa H, Gurses-Ozden R, Buxton D, Ritch R. Acute conformational changes in the optic nerve head with rapid intraocular pressure elevation: implications for LASIK surgery. *Ophthalmic Surg Lasers Imaging* 2003;34:334-341.
25. Davies LN, Bartlett H, Mallen EA, Wolffsohn JS. Clinical evaluation of rebound tonometer. *Acta Ophthalmologica* 2006;84:206-209.
26. Thirion J-P. Image matching as a diffusion process: an analogy with Maxwell's demons. *Med Imaging Anal* 1998;2:243-260.
27. Armstrong RA. When to use the Bonferroni correction. *Ophth Phys Opt* 2014;34:502-508.
28. Sigal IA, Flanagan JG, Tertinegg I, Ethier CR. Modeling individual-specific human optic nerve head biomechanics. Part I: IOP-induced deformations and influence of geometry. *Biomech Model Mechanobiol* 2009;8:85-98.
29. Sigal IA, Flanagan JG, Tertinegg I, Ethier CR. Modeling individual-specific human optic nerve head biomechanics. Part II: influence of material properties. *Biomech Model Mechanobiol* 2009;8:99-109.

30. Girard MJ, Tun TA, Husain R, et al. Lamina cribrosa visibility using optical coherence tomography: comparison of devices and effects of image enhancement techniqueslamina cribrosa visibility in OCT. *Invest Ophthalmol Vis Sci* 2015;56:865-874.

FIGURE CAPTIONS

Figure 1 – Schematic representation of the time course for each experimental run. For baseline runs, the target force was zero.

Figure 2 – A. Relationship between central corneal thickness and corneal hysteresis. B. Relationship between central corneal thickness and baseline IOP. C. Relationship between corneal hysteresis and baseline IOP.

Figure 3 – Effect of IOP elevation on displacement of optic nerve tissue assessed using SLO. Representative images collected at baseline (A) and during IOP elevation (B) are shown overlaid with manual segmentation of structures. The horizontal and vertical displacement of the vessel edge (green trace) and the cup edge (blue trace) are expressed as a difference from the respective displacement of the disc (red trace). C. Relationship between baseline IOP and horizontal displacement of the cup edge. D Relationship between IOP elevation and horizontal displacement of the cup edge. E. Relationship between central corneal thickness and vertical displacement of the cup edge. F. Relationship between corneal hysteresis and vertical displacement of the cup edge. Values represent the average for three masked manual graders.

Figure 4 – Effect of IOP elevation on displacement of optic nerve tissue assessed using SLO. A. Representative tissue displacement for six participants, demonstrating heterogeneity in tissue response to IOP elevation. Colour bar shows magnitude of displacement in microns. B. Relationship between corneal hysteresis and cup:disc displacement ratio. C. Relationship between corneal hysteresis and cup:disc displacement ratio.

Figure 5 – Effect of IOP elevation on displacement of optic nerve tissue assessed using OCT. Representative images collected at baseline (A) and during IOP elevation (B) are shown overlaid with manual segmentation of structures. Displacement of the optic nerve surface (red trace) and the anterior lamina cribrosa (blue trace) are expressed as a difference from Bruch's membrane measured at a peripheral location 1.5 mm from the optic

nerve (green 'r'). C. Relationship between central corneal thickness and anterior lamina cribrosa displacement. D Relationship between corneal hysteresis and lamina cribrosa displacement. E. Relationship between anterior lamina cribrosa displacement and vertical displacement of the cup edge. F. Relationship between anterior lamina cribrosa displacement and vertical displacement of the vessel edge. Values represent the average for three masked manual graders.

Table 1: Baseline data for experimental participants.

	Mean (SD)	**Range**
Age (yrs)	33.3 (6.8)	22.6 – 46.9
Sex (F:M)	12:9	
Axial length (mm)	23.9 (1.7)	22.5 – 28.9
Baseline IOP (mmHg)	13.7 (3.8)	8 – 23
Change in IOP (mmHg)	12.0 (4.2)	7 – 22
CCT (mm)	558 (43)	478 629
Corneal Hysteresis	10.5 (1.2)	8.3 – 12.9

Table 2: Summary statistics for distribution of tissue displacement (top row), correlations between baseline parameters and tissue displacement (middle rows) and correlations between laminar displacement and other measured displacements (bottom row).

	vessel edge (Δx µm)	**cup edge** (Δx µm)	**vessel edge** (Δy µm)	**cup edge** (Δy µm)	**ant. LC** (Δz µm)	**ONH surf.** (Δz µm)	**within-disc** (av. Δr µm)	**cup:disc** (ratio)
mean ± SD **range**	-20 ± 28 (-93, +18)	-3 ± 33 (-62, +35)	2 ± 29 (-74, +58)	0 ± 34 (-81, +46)	-15 ± 19, (-60, +17)	-9 ± 11 (-34, +12)	20 ± 9 (+7, +48)	1.8 ± 0.9 (0.5, 4.2)
baseline IOP R^2, p-value y = mx + c	0.07, 0.25	0.33, 0.006 3.6x -52	<0.01, 0.94	0.02, 0.54	<0.01, 0.85	0.01, 0.61	0.13, 0.10	0.09, 0.18
IOP elevation	0.09, 0.18	0.43, 0.001 -3.6x +40	0.01, 0.66	0.03, 0.66	0.04, 0.37	<0.01, 0.84	0.04, 0.40	0.02, 0.59
central corneal thickness	<0.01, 0.88	0.08, 0.25	0.12, 0.15	0.35, 0.007 -0.48x +270	0.08, 0.24	0.12, 0.14	0.06, 0.32	0.39,0.004 0.01x -5.9
corneal hysteresis	<0.01, 0.74	0.05, 0.32	0.12, 0.12	0.12, 0.24	<0.01, 0.85	0.05, 0.34	0.02, 0.58	0.10, 0.16
anterior lamina cribrosa	<0.01, 0.98	0.08, 0.20	<0.1, 0.79	0.25, 0.02		0.08, 0.21	0.03, 0.45	<0.01, 0.98

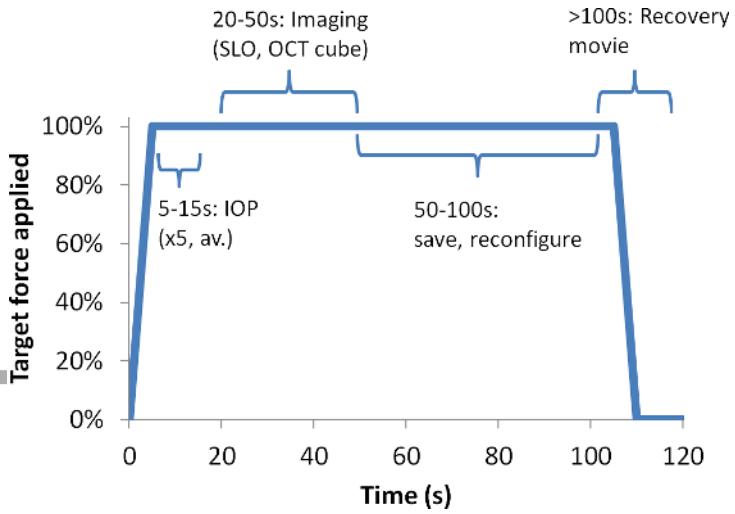

opo_12568_f1.tif

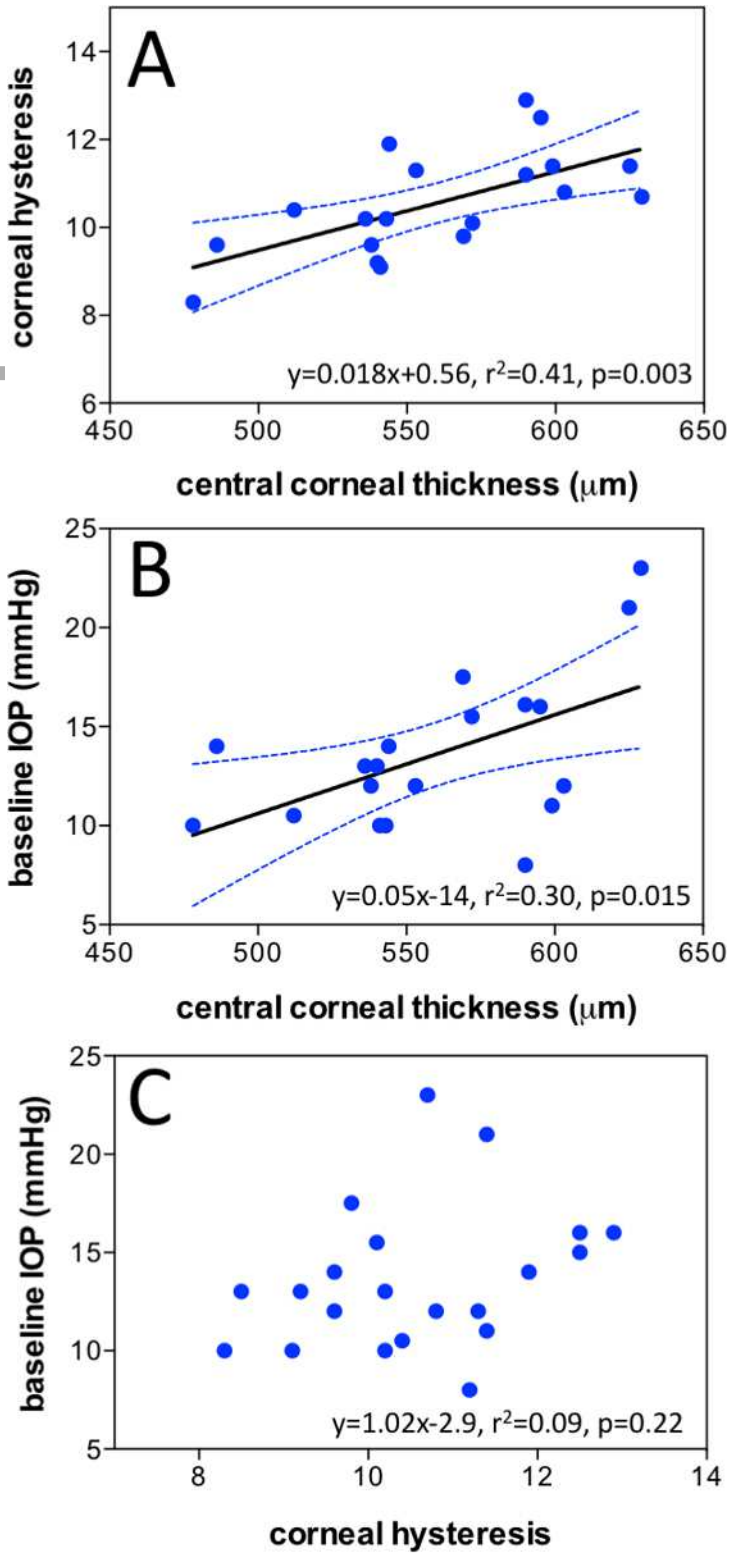

opo_12568_f2.tif

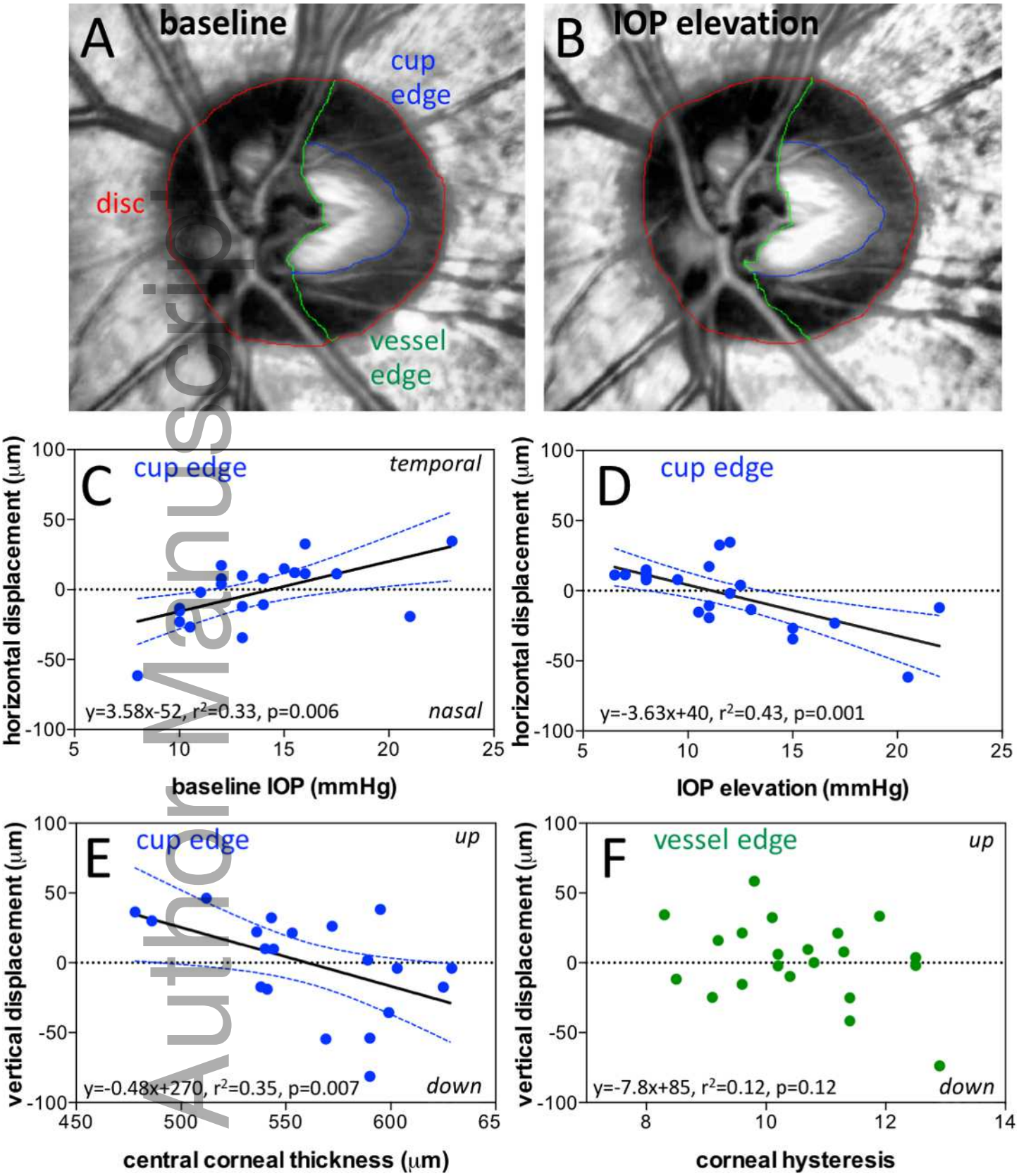

opo_12568_f3.tif

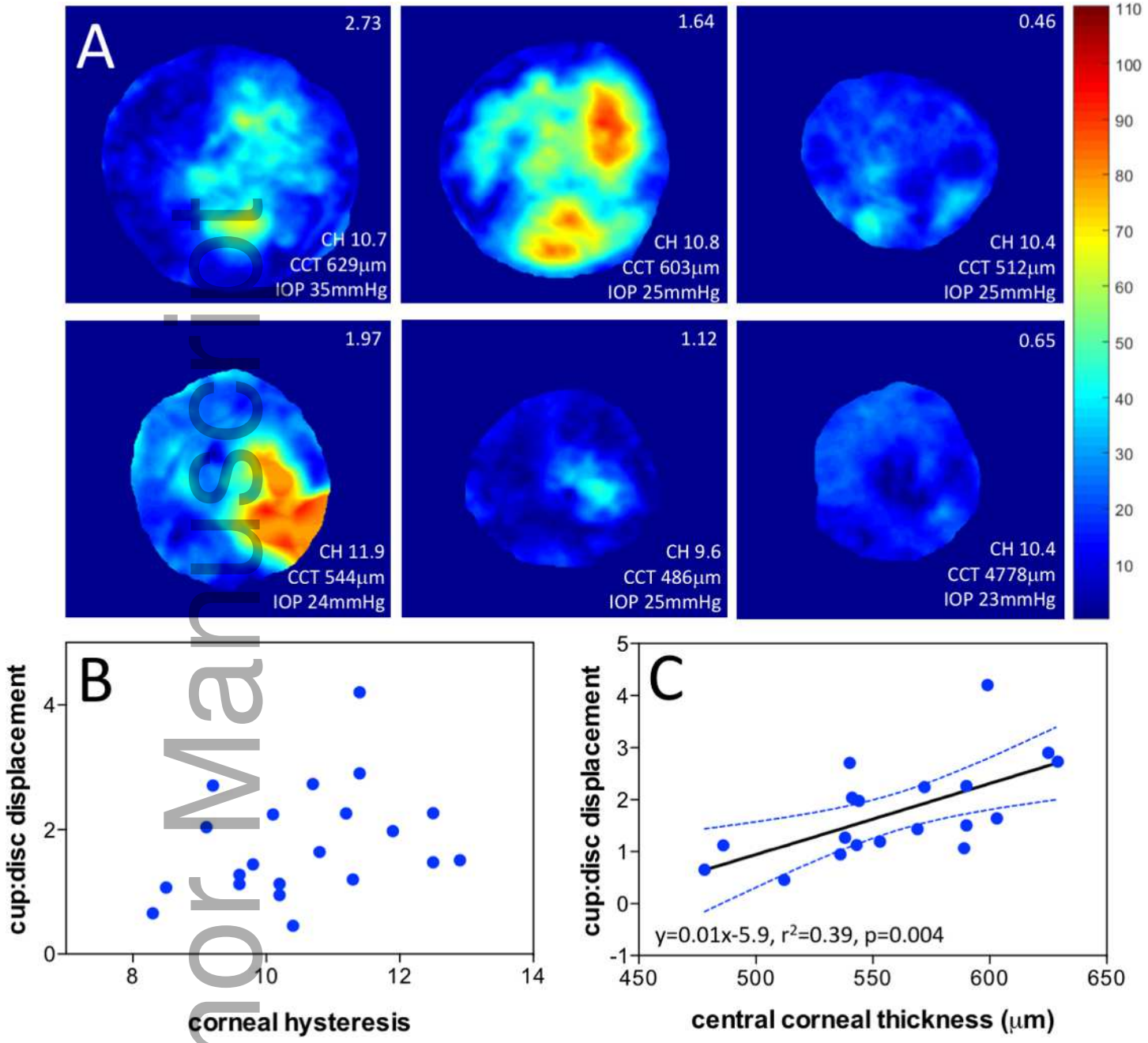

opo_12568_f4.tif

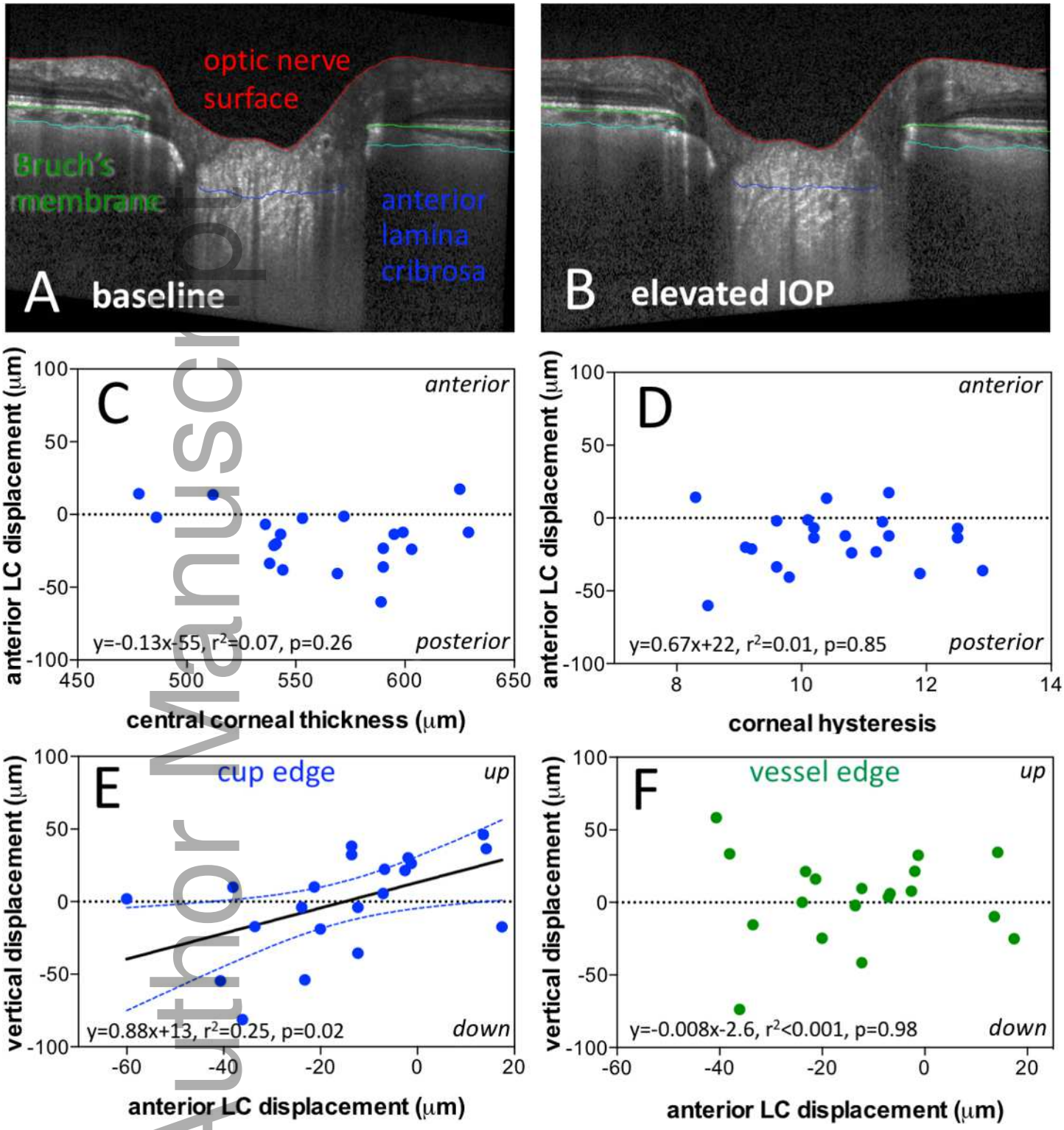

opo_12568_f5.tif